CONF-811113--26

LA-UR-81-3027

MASTER

TITLE: Automated Computer Analysis of X-Ray Radiographs Greatly Facilitates Measurement of Coating-Thickness Variations in Laser-Fusion Targets

AUTHOR(S): D. M. Stupin, K. R. Moore, G. D. Thomas, R. L. Whitman

SUBMITTED TO: For presentation at the American Vacuum Society 28th National Symposium, Anaheim, California November 3-6, 1981

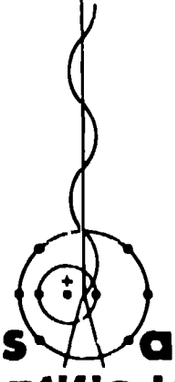

los alamos
scientific laboratory
of the University of California
LOS ALAMOS, NEW MEXICO 87544

Form No. 836
St. No. 2629
1/5

UNITED STATES
ENERGY RESEARCH AND
DEVELOPMENT ADMINISTRATION
CONTRACT W-7405-ENG-36

Automated Computer Analysis of X-Ray Radiographs Greatly Facilitates Measurement of Coating Thickness Variations in Laser Fusion Targets

D. M. Stupin, K. R. Moore, G. D. Thomas, R. L. Whitman
Los Alamos National Laboratory, University of California
Los Alamos, NM 87545

Abstract

We have built an automated system to analyze x-ray radiographs of laser fusion targets which greatly facilitates the detection of coating thickness variations. Many laser fusion targets require opaque coatings 1 to 20 μm thick which have been deposited on small glass balloons 100 to 500 μm in diameter. These coatings must be uniformly thick to 1% for the targets to perform optimally. Our system is designed to detect variations as small as 100 Å in 1-μm-thick coatings by converting the optical density variations of contact x-ray radiographs into coating thickness variations. Radiographic images are recorded in HRP emulsions and magnified by an optical microscope, imaged onto television camera, digitized and processed on a Data General S/230 computer with a code by Whitman. After an initial set-up by the operator, as many as 200 targets will be automatically characterized.

Automated Computer Analysis of X-Ray Radiographs Greatly Facilitates Measurement of Coating Thickness Variations in Laser Fusion Targets

D. M. Stupin, K. R. Moore, G. D. Thomas, R. L. Whitman
Los Alamos National Laboratory, University of California
Los Alamos, NM 87545

INTRODUCTION

We have built an automated system to analyze x-ray radiographs of laser fusion targets at the Los Alamos National Laboratory which greatly facilitates the detection of coating thickness variations in these targets. The Microradiographic Analysis System (MIRAS - from the Spanish look) is sensitive to 1% variation in coating thickness for Type-I and Type-II defects, and, therefore, meets the requirements imposed by target designers for these two types of defects. We have proven the accuracy and sensitivity of this system by direct comparision with data taken with a flatbed microdensitometer and optical interference measurements. The on-line processing features of MIRAS give fast turn-around time for the analysis of the targets and the automated features of the system mean that the operator is not required to devote his attention full-time to the analyses.

Laser fusion targets are typically hollow glass microballoons 100 to 500 μm in diameter, coated with 1- to 20-μm-thick layers of various plastics and metals. While the glass microballoons are transparent, it is usually not practical to measure the coating uniformity or the coating thickness with optical techniques, because the coatings are usually opaque. However, the uniformity of the microballoon wall and the subsequent coatings must be stringently controlled to guarantee the performance of the targets. X-ray radiography has been shown to be effective in detecting target defects in opaque and transparent coatings,[1-9] and we are developing the most sensitive methods to find these defects with x-rays.

Coating thickness variations are detected by measuring x-ray transmission through the targets as shown in Fig. 1. X-rays incident

from the top of the figure pass through the asymmetric microballoon and expose the film underneath the microballoon. However, the intensity of the x-rays is attenuated exponentially by the amount of the material they pass through. Hence, the x-ray flux to the center of the balloon is not attenuated as much as the flux near the left or right edge. When the optical density of the radiographic image is plotted along the image diameter, as shown at the bottom of the figure, one typically gets cup-shaped plots. Furthermore, because of the asymmetry of the microballoon, the cup rim is higher on the left side of the plot than it is on the right side. This asymmetry in the optical density plot can be detected by a computer and quantified.

APPARATUS

MIRAS uses a television camera to digitize the radiographic image of a target as shown in Fig. 2. First, a contact microradiographic image is made in photographic emulsion with an x-ray source. This image is placed on the computer-controlled x-y stage and viewed in the microscope by a television camera. The video signal is digitized, this digital data is stored in the computer, and the computer searches the digital data for defects and prints the results of the search. Up to 200 images in a single radiographic array will be analyzed automatically without further assistance after the operator has indicated the location of the images and assigned identification numbers. The computer prints the identification, microballoon diameter, thickness of the coating, nonconcentricity (Type-I defect), ellipticity (Type-II defect), and volumes of the Type-III defects for each image. A more detailed description of this process is in the appendix.

PERFORMANCE

MIRAS meets the requirements of inertial confinement fusion target designers for sensitivity to Type-I and Type-II defects. We have arbitrarily divided the types of defects typically found in microballoons and coatings into three types which are shown in Fig. 3 The Type-I defect is a nonconcentricity between the outer and inner surface, a Type-II is an elliptical inner or outer surface, or both, and Type-III is a small local defect such as a wart or a dimple, on either surface, or a

density variation in the coating. Target designers have estimated that Type-I or Type-II Defects smaller than 1% in $\Delta t/t$ will not degrade target performance, where t is the average coating thickness and Δt is the variation about the average. Defects of Type-III must be smaller than 0.1% in $\Delta t/t$ if they cover an area of t^2. MIRAS is sensitive to 1% Type-I defects and 2% Type-II.

The accuracy of MIRAS is proven by comparison with flatbed densitometer data and optical interference measurements. In Fig. 4 are shown the measured nonconcentricities in percent $\Delta t/t$ for eleven microballoons which were analyzed with data taken with both a flatbed densitometer and with MIRAS. Ten of these microballoons are transparent and were also measured with optical interferometric techniques in the same orientation as in the radiographic analyses. In all cases the measurements differ by less than 4% in wall thickness.

The on-line processing capability of MIRAS gives us one day turn-around time for the analyses. Each radiographic array requires about 30 minutes to set up and each image in the array requires 25 minutes for processing. Therefore, to characterize three views of a five-microballoon array, about two-and-a-half hours are required for each view, and each target will be competely characterized in less than eight hours, giving one day turn-around. We expect to reduce the time required for each image to fifteen minutes by improving the software.

CONCLUSION

The automated analysis features of MIRAS do not require a full time operator. In the example just cited the operator need only spend thirty minutes to set up each view and has the other six hours to devote to other tasks. Furthermore, arrays containing as many as 200 targets can be set up and left to run without further operator assistance. Hence, a thirty-target array could be set up in the evening and left to be analyzed overnight. Such an array would require only forty-five minutes for set-up.

The automated computer analysis of x-ray radiographs of laser fusion targets at the Los Alamos National Laboratory greatly facilitates the measurement of coating thickness variation in these targets. MIRAS meets

the requirements of the inertial confinement fusion target designers for sensitivity to Type-I and Type-II defects. Its accuracy is proven by direct comparison with data taken with a flat-bed densitometer and optical interference measurements. The on-line processing capability gives it fast turn-around capability, and the automated analysis features of MIRAS do not require a full time operator and free the operator for other tasks.

APPENDIX

MIRAS uses a television camera to digitize the radiographic image of a target as shown in Fig. 2. First, a contact microradiographic image is made in photographic emulsion with an x-ray source. This image is placed on the computer-controlled x-y stage and viewed in the microscope by a television camera. The video signal is digitized, this digital data is stored in the computer, and the computer searches the digital data for defects and prints the results of the search. Up to 200 images in a single radiographic array will be analyzed automatically without further assistance after the operator has indicated the location of the images and assigned identification numbers. The computer prints the identification, microballoon diameter, thickness of the coating, nonconcentricity (Type-I defect), ellipticity (Type-II defect), and volumes of the Type-III defects for each image.

The contact microradiographic image is made with either a monoenergetic[10] or bremsstrahlung x-ray source with a geometric unsharpness in the image of 0.02 d or less for a point on the equator of the target parallel to the film plane, where d is the diameter of the microballoon. The targets are placed in arrays on 4-μm-thick mylar films to make it easier to move them in the x-ray laboratory, and these arrays are placed directly on either Kodak High Resolution Plates, Type 2A, or Kodak High speed Holographic Plates, Type 131 02 photographic emulsions during an exposure. These arrays contain up to 200 targets. To determine the coating thickness, a penetrameter or step wedge of approximately the same material and thickness as the coating is placed next to each array during the exposure. The optical density in the center of each target image is compared to the optical densities of the penetrameter, and the coating thickness is calculated by interpolation. Of course, one radiographic image contains information about only one view of the target, and to completely characterize each target three orthogonal views are made.[11]

The microscope[12] has a halogen light source that is powered by a 10V-10A regulated power supply[14] to stabilize the illumination intensity.

We have evaluated three television cameras for use with MIRAS by comparing their performance to a Photometric Data Systems flatbed densitometer[13]. The three cameras are a Fairchild MV-201,[15] an Image Technology Methods (ITM) 201/E Densitometric,[16] and a Fairchild CCD2000.[17] Both the Fairchilds use a charge-coupled device (CCD) which is an array of silicon detectors mounted on single integrated circuit chip as the light sensor while the ITM camera uses a vidicon tube. All three produce a (nearly) standard video signal.

The video signal is digitized into a 256x256 picture elements (pixels) with an 8-bit analog-to-digital converter.[18] It requires about 10 seconds to digitize an image, and it has a scan converter to display images in computer memory on a standard video screen.

Digitized data is stored and processed in a Data General S/230[19] minicomputer with 192K words of memory and two 10 mega-byte magnetic disks.

The computer program is divided into two parts: (1) digitization and correction of the image, and (2) the computer analysis for defects. To prepare the digitized image for defect analysis, three corrections and two calibrations are performed. Corrections are made for dirt in the optics, field flatness, and rectangularity.

Corrections for dirt in the microscope or television optics and pixels in the video sensor which are not light sensitive are done in the following manner: a flat field with an optical density about equal to the optical density in the center of the microballoon images is digitized and the average and the standard deviation of the distribution of the optical densities of the pixels are calculated. Locations of pixels with optical densities which differ by more than three or four times the standard deviation from the average are put in a bad pixel file. When analyzing a microballoon image, the digitized values of these bad pixels are replaced with the average value of the nearest good pixels above and below them in a vertical scan line. We plan to replace this crude correction with a better scheme.

We perform a field flattening correction to remove variations in the response to incident light over the surface of the television sensor and

light intensity variations due to the microscope optics. These can cause a field with uniform optical density on the microscope stage to appear to have a nonuniform optical density in the digitized computer image. For this correction, we map the television response to three and as many as ten flat fields that have optical denities that span the range of optical densities found in the radiographic microballoon images. On a pixel-by-pixel basis this response is fit to the optical density of the fields by a quadratic equation. The three coefficients from the quadratic fit are stored and used to correct the data from each microballoon image. Locations of any pixels whose response cannot be fit with a coefficient of determination (often called r^2) larger than 0.95 are added to the bad pixel file.

A standard video image that appears rectangular on a TV screen appears to be a square image in the computer, and, therefore, a round microballoon image appears to be a vertically oblong object to the computer. Hence, we stretch the image horizontally with a bilinear interpolation so that the computer will see a round object.

Two calibrations are performed to ensure that MIRAS gives accurate and sensitive results, one to convert the digital data of the video image to optical density, and another to convert optical density to a known thickness of material using the penetrameter image. Conversion of the digital data to optical density is done in the flatfield correction, already described, by fitting each pixel response to the optical density of a known neutral density filter. Once the optical density conversion is known, the average and the standard deviation of the optical densities of the pixels in the image of each penetrameter step are calculated. Average optical densities are used in a look-up table to convert optical density to thickness of material by linear interpolation. Standard deviations, s, are used to fit the equation

$$s = cD^a,$$

where c and a are constants to be fit and D is the average optical density. These parameters are used in the analysis code [2,4,20] to determine the significance of Type-III defects.

The computer code to find the coating thickness variations was written by Whitman for a CDC 7600 computer and converted by Thomas to run on a Data General S/230 Eclipse. On the Eclipse, the code has two versions, one which processes images which are as large as 256 x 256 pixels and another which can process images as large as 1024 x 1024 pixels. Because of the limited memory in the Eclipse, the latter version uses many more disk files than the former version, and the time needed to access these files causes the second version to run longer than the former. All of the results presented here were produced using the 256 x 256 version which takes about 10-15 minutes to run per image, depending on the number of Type-III defects that are found. Both versions are sensitive to Type-I, -II, and -III defects. Although the sensitivity to Type-III defects is impressive, Whitman has shown[2,4] that it is not nearly as good as the target designers require.

Whitman demonstrated the accuracy and sensitivity of his code in Refs. 2,4,20. Thomas's version is proven to be completely equivalent to the earlier version by direct comparison. Eight computer-simulated microballoons were processed on both the CDC 7600 and the Eclipse. The answers from the two versions agree to within 3% in coating thickness.

By direct Comparison, MIRAS, using a television camera to digitize radiographic images, has been shown to be as sensitive to Types I and II defects as another system that uses a flatbed microdensitometer. We expect that changes in the MIRAS software will produce equivalent results for Type-III defects, as well as shortening the analysis time.

References

1. T. M. Henderson, D. E. Cielaszyk, and R. J. Simms, Rev. Sci. Instrum. 48, 835 (1977).
2. R. L. Whitman and R. H. Day, Appl. Opt. 19, 1718 (1980).
3. H. J. Trussell, Appl. Opt. 19, 3587 (1980).
4. R. L. Whitman, R. H. Day, R. P. Kruger, and D. M. Stupin, Appl. Opt. 18, 1266 (1979).
5. R. M. Singleton, B. W. Weinstein, and C. D. Hendricks, Appl. Opt. 18, 4116 (1979).
6. R. M. Singleton, D. E. Perkins, D. L. Willenborg, and G. A. Gleeson, in Digest of Topical Meeting on Inertial Confinement Fusion (Optical Society of America, Washinton, D.C., 1980), paper THE-2.
7. R. H. Day, T. L. Elsberry, R. P. Kruger, D. M. Stupin, and R. L. Whitman, in Eighth International Conference on X-Ray Optics and Microanalysis (Science Press, Princeton, NJ, 1979), pp. 275-282.
8. G. M. Halpern, J. Varon, D. C. Leiner, and D. T. Moore, J. Appl. Phys. 48, 1223 (1977).
9. R. M. Singleton and J. T. Weir, J. Vac. Sci. Technol. 18, 1264 (1981).
10. D. M. Stupin, M. A. Winkler, R. H. Day, C. K. Crawford, and T. S. Tyrie, in Digest of Topical Meeting on Inertial Confinement Fusion (Optical Society of America, Washington, DC, 1980), Paper THB-19.
11. R. M. Singleton, C. D. Hendricks, and B. W. Weinstein in Digest of Topical Meeting on Inertial Confinement Fusion (Optical Society of American, Washington, DC, 1978), Paper TUE10.
12. Universal Model, Carl Zeiss, New York ,NY
13. Photometric Data Systems, Perkin-Elmer Div., Boller and Chivens, South Pasadena, CA.
14. Model SRL 20-25, Sorenson Co., Manchester, NH
15. Fairchild Camera and Instrument Corp., Imaging Systems Div., Syosset. NY. This device is no longer available.
16. Image Technology Methods Corp., Sudbury, MA
17. Fairchild CCD Imaging, Palo Alto, CA.
18. Model 300 Graphic Memory, Vidco, Portland, OR
19. Data General Corp., Westboro, MA
20. R. L. Whitman, "An Efficient Method That Precisely Characterizes Laser Target Defects More Complex Than Nonconcentricity," submitted to this conference

FIGURE CAPTIONS

Fig. 1 Coating thickness variations are detected by measuring x-ray transmission through the targets. The images are recorded in photographic emulsions, and the optical densities of the emulsions are a measure of the transmitted x-ray flux. Therefore, coating thickness variations are detected as variations in the optical density. In this example, an asymmetric microballoon gives an unsymmetric optical density plot.

Fig. 2 Miras uses a television camera to digitize radiographic images. Contact microradiographs are placed on the computer-controlled x-y stage and viewed through the microscope by a television camera. The video images are digitized and stored in computer memory where an analysis program calculates the sizes of defects and prints the results.

Fig. 3 Three types of defects are found in microballoons. Type-I defects are nonconcentricities between the inner and outer surfaces. Type-II is an elliptical inner or outer surface (or both). Type-III are warts or dimples in either surface, or cracks or voids in the coating or density variations in the coating.

Fig. 4 The accuracy of MIRAS is proven by direct comparison with flatbed densitometer data (hatched) and optical interferometric measurements (shaded) for eleven different microballoons. In each case, all the measurements agree to within $\pm 4\%$ in absolute coating thickness.

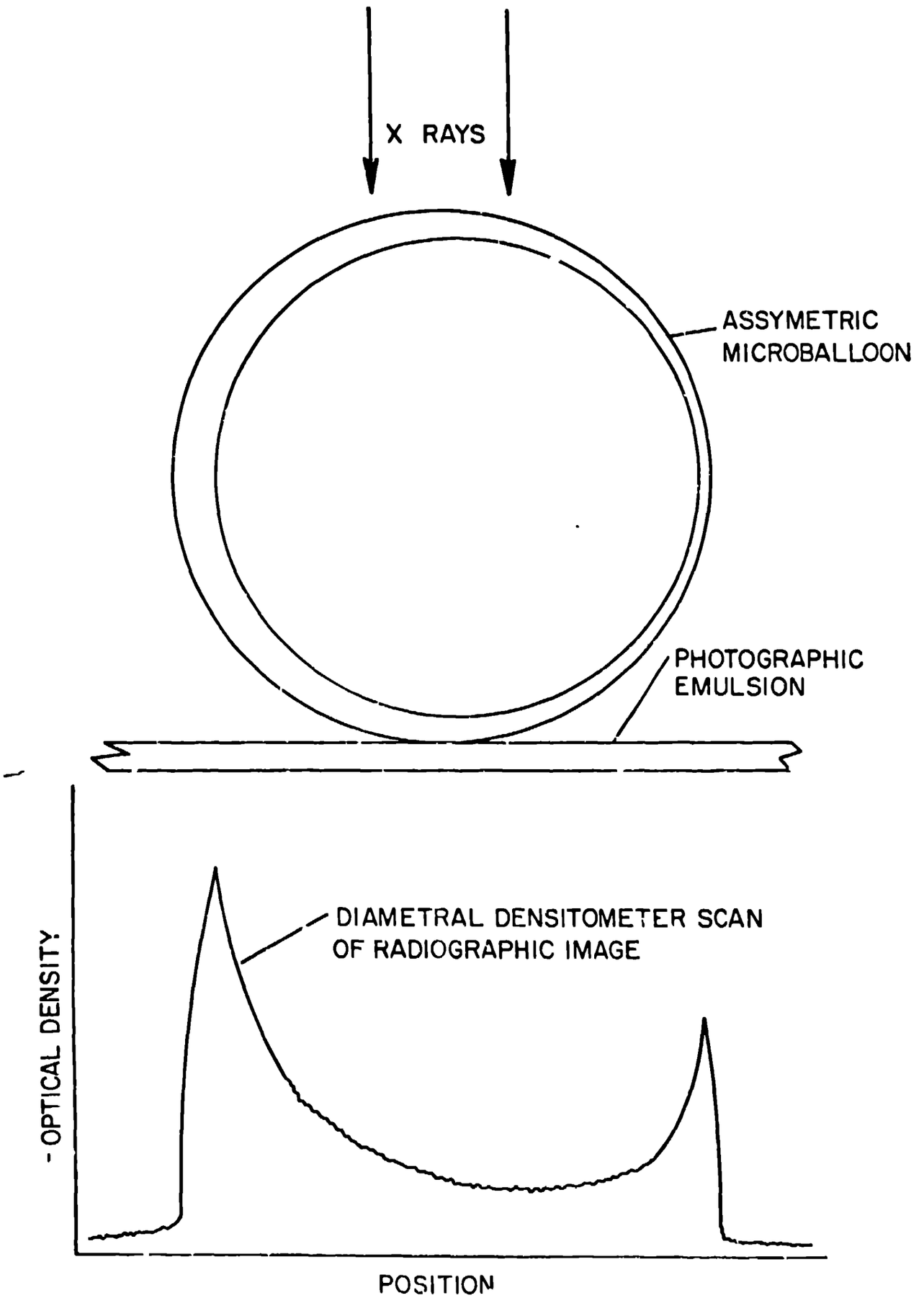
X RAYS
ASSYMETRIC
MICROBALLOON
PHOTOGRAPHIC
EMULSION
DIAMETRAL DENSITOMETER SCAN
OF RADIOGRAPHIC IMAGE
- OPTICAL DENSITY
POSITION

Fig. 1

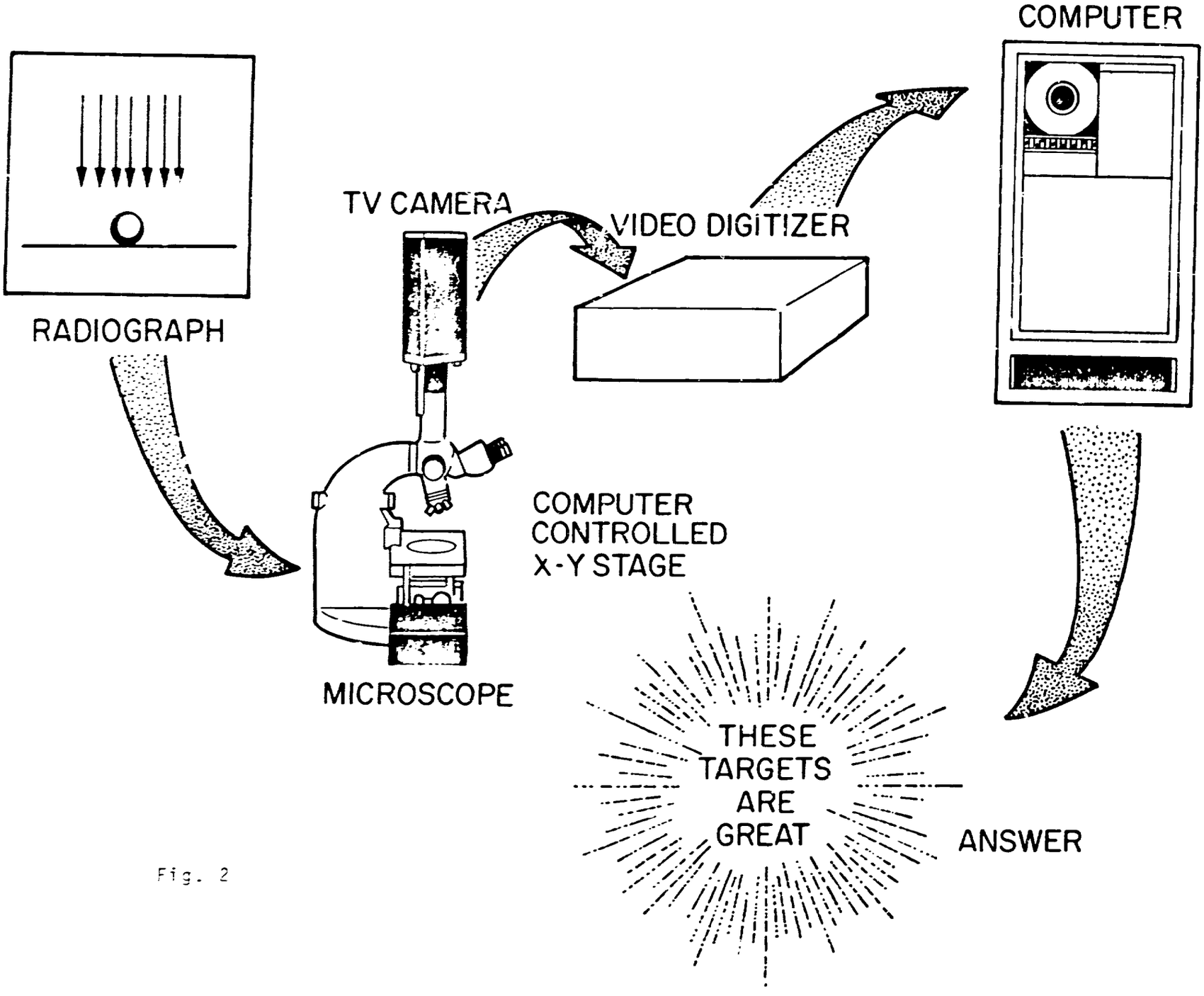
COMPUTER
TV CAMERA
VIDEO DIGITIZER
RADIOGRAPH
COMPUTER
CONTROLLED
X-Y STAGE
MICROSCOPE
THESE
TARGETS
ARE
GREAT
ANSWER

Fig. 2

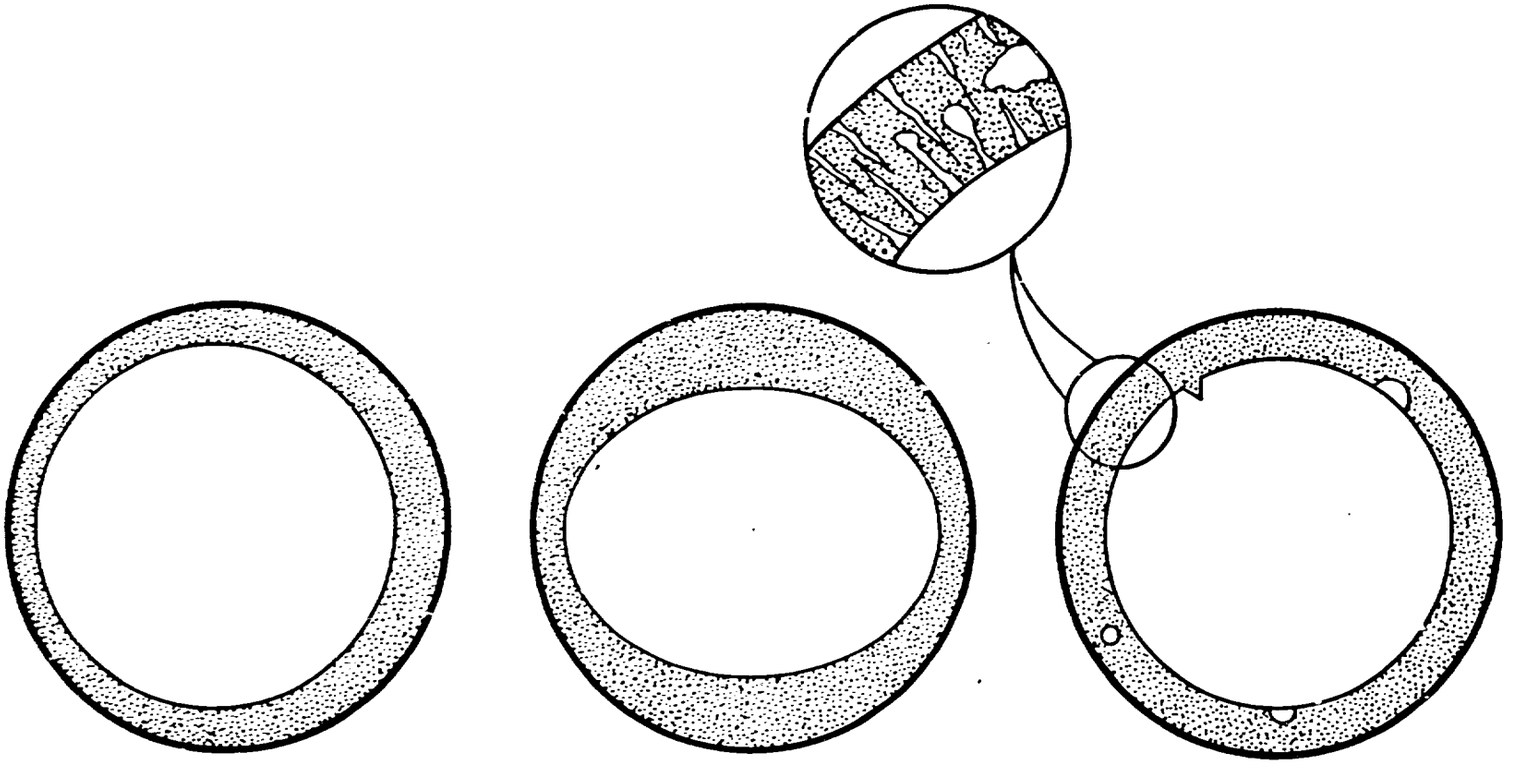

Fig. 3

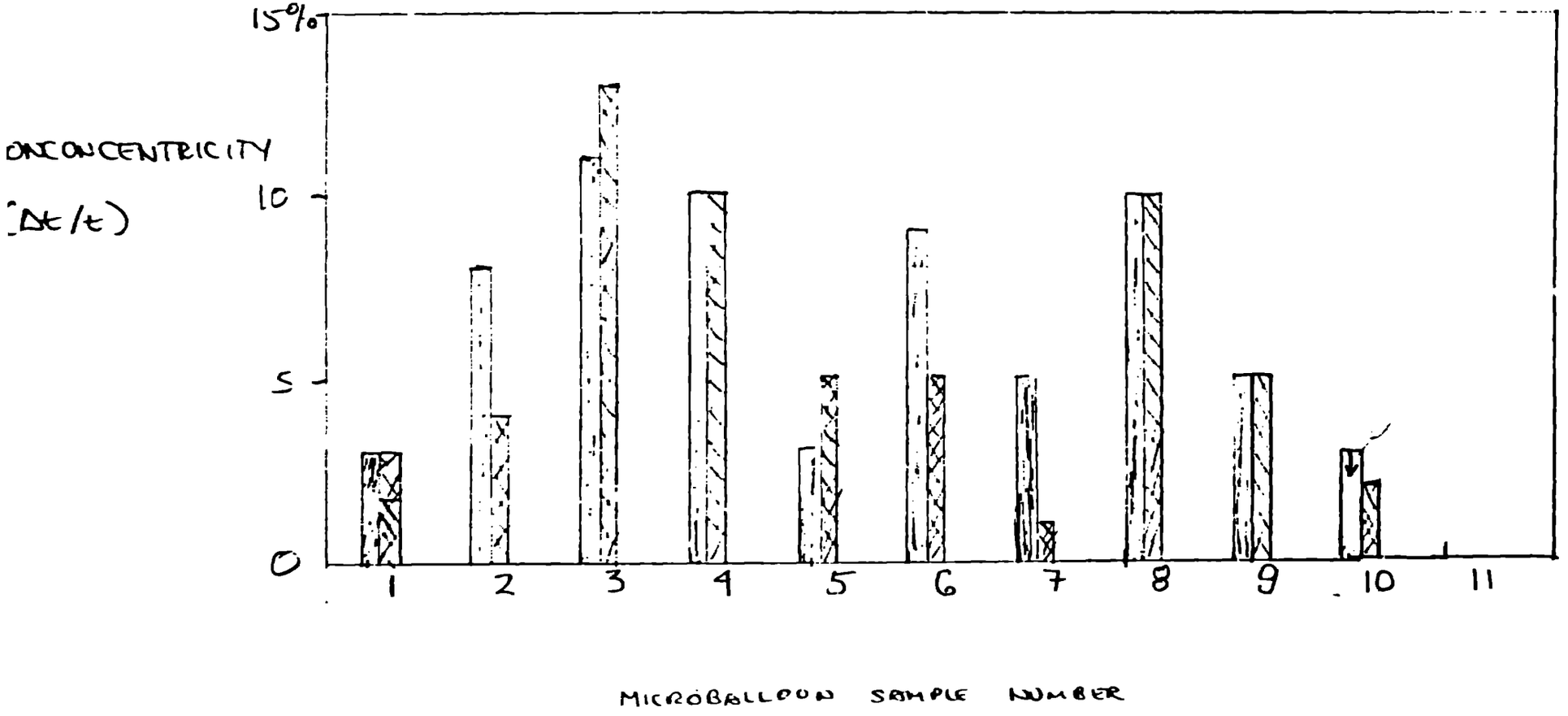

Fig. 4 (typical)